Ain Shams Engineering Journal 15 (2024) 102675

Contents lists available at ScienceDirect

Ain Shams Engineering Journal

journal homepage: www.sciencedirect.com

Full Length Article

A robust modified notch filter based SOGI-PLL approach to control multilevel inverter under distorted grid

Praveen Bansal [a], Shishir Dixit [a], Saket Gupta [b], Majed A. Alotaibi [c,*], Hasmat Malik [d,f,*], Fausto Pedro García Márquez [e,*]

[a] Electrical Engineering Department, Madhav Institute of Technology and Science, Gwalior, India
[b] Instrumentation and Control Engineering Department, Bharati Vidyapeeth's College of Engineering, New Delhi 110063, India
[c] Department of Electrical Engineering, College of Engineering, King Saud University, 11421, Saudi Arabia
[d] Department of Electrical Power Engineering, Faculty of Electrical Engineering, Universiti Teknologi Malaysia (UTM), Johor Bahru 81310, Malaysia
[e] Ingenium Research Group, Universidad Castilla-La Mancha, 13071 Ciudad Real, Spain
[f] Department of Electrical Engineering, Graphic Era (Deemed to be University), Dehradun 248002, India

ARTICLE INFO

Keywords:
Power quality
Shunt active power filter
Multilevel inverter
Adaptive control

ABSTRACT

This paper introduces a novel approach to enhance the control algorithm for a single-phase shunt active power filter(SAPF) by integrating a new technique into a 5-level cascaded multilevel inverter (MLI) with Photo Voltaic (PV) array integration. Due to the integration of non-linear loads in the grid, such as computers, variable speed drives, and other solid-state equipment, non-sinusoidal currents are drawn, introducing harmonics that distort the voltage and current waveforms. It is essential to mitigate these harmonics, and integrating Shunt Active Power Filters (SAPFs) gives the grid the ability to inject active power. In order to improve power quality and achieve active and reactive power balance, this integration requires an imperative control method. This work extracts the fundamental component of the load current and efficiently handles grid distortions such as DC offset, phase shift, and harmonics using a phase lock loop (PLL) based on a Modified Notch Filter Second Order Generalised Integrator (MNFSOGI). Using MATLAB/Simulink software modelling, experimental validation utilising the OPAL-RT real-time data simulator verifies the proposed system's operation. The control algorithm, which has been painstakingly designed and verified, allows feed-forward current estimate from the PV array, synchronization template obtained from the grid voltage signal, and estimation of both fundamental and non-linear load currents. The performance of the MNFSOGI-PLL is additionally compared with that of the conventional E-PLL, MAF-PLL and DSOGI-PLL techniques. By attaining power balance in multilevel inverters under distorted grid conditions, this research substantially contributes to improving power quality. According to simulation and experimental results, the Total Harmonic Distortion (THD) of the grid current is found to be 1.50% in normal grid and 3.96% in distorted grid which is less than 5%, by IEEE-1547 standards. Moreover, the limitations of the presented multilevel inverter system are highlighted by the disadvantages of traditional 2-level inverters, which include increased harmonics, restricted voltage levels, and poorer power quality.

1. Introduction

Power generation has undergone a discernible shift in recent years, shifting from conventional techniques to renewable energy sources (RES). This change is mostly caused by the need to reduce carbon emissions, the steady depletion of conventional energy sources, and the goal of producing power at the distribution level in order to reduce power losses via large transmission networks presented by Hossain *et al.* [1]. The abundance of sunlight and the ability of the Solar Photovoltaic (SPV) system to generate power with zero carbon emissions have made it stand out among the different predicted RES. Among the several anticipated RES, the Solar Photovoltaic (SPV) system stands out due to its abundance of sunshine and ability to create power with zero carbon emissions. In order to guarantee increased dependability and the high quality of the electrical grid, PV inverters must abide by strict grid-integration standards when there is a significant injection of renewable energy sources into the system, according to research by Hossain *et al.* [2], the IEEE Application Guide [3], and the work by Kirmani et al.

* Corresponding authors.
E-mail addresses: MajedAlotaibi@ksu.edu.sa (M.A. Alotaibi), hasmat.malik@gmail.com (H. Malik), faustopedro.garcia@uclm.es (F. Pedro García Márquez).

https://doi.org/10.1016/j.asej.2024.102675
Received 13 October 2023; Received in revised form 28 December 2023; Accepted 24 January 2024
Available online 13 February 2024

[4]. For instance, according to the updated IEEE drafts, the current supplied by grid-connected PV systems (utility grid current) must be constantly balanced, sinusoidal, and its total harmonic distortion (THD) must be kept below 5 %0.1547 and 519-2014.

More specifically, the benefit of effectively using generated power is provided by the grid-connected Solar Photovoltaic (SPV) power conversion system. This is significant because the main shortcoming of SPV systems is that they can only meet load demands on sunny days. It becomes essential to integrate the SPV system with the conventional distribution network once this constraint is acknowledged. According to Mejdar, Salimi, and Zakipour *et al.* [5], this integration guarantees a constant power supply throughout the day in addition to improving system performance overall. Using a voltage-sourced inverter (VSI) allows Renewable Energy Sources (RES) to be integrated into the distribution system.

In the present situation, the proportion of non-linear loads in power distribution systems has increased noticeably. These non-linear loads frequently produce non-sinusoidal currents, which have a negative effect on the overall performance and control of the system. To address these difficulties, it is crucial to create efficient control algorithms for grid-integrated PV inverters. The literature has numerous examples of control methods that have been developed in both the frequency and time domains. These methods seek to extract the active component of the load current, improving power quality (PQ) as presented by F. Blaabjerg *et al.* [6]. Some of the authors have presented the hybrid system for standalone system by A. Naderipour et al. [7]. The Stability and dynamic analysis of PV integrated PV system is presented by Naderipour et al[8]. A design framework for an annually loaded grid-connected photovoltaic-wind energy system with battery storage (PV/Wind/Battery) is executed to achieve optimal configuration is discussed by H. Kamyab et al. [9] and A. Naderipour et al. [10] have presented the An innovative design framework is proposed for a standalone and grid-connected hybrid renewable energy system incorporating photovoltaic, wind, and battery components. The framework takes into account considerations of reliability, cost, and emissions.

B.Singh *et al.* [11] have put forth numerous solutions, including shunt active power filters (SAPF), distribution static compensators (DSTATCOM), dynamic voltage restorers (DVR), and series-shunt compensators such unified power quality conditioners (UPQC), have been developed as a result of the development of custom power devices. These techniques are intended to lessen the drawbacks of passive filters.SAPF is one of the foremost technologies available in literature presented by Mahela OP *et al.* [12] to counter these PQ problems.

A key element in the SAPF's architecture is the inverter unit. The low-voltage distribution industry frequently uses two-level inverters. When designing SAPFs for the medium-voltage (MV) to high-voltage (HV) distribution industry, design engineers now instinctively use Multi-Level Inverters (MLIs). Benefits of MLIs include lessened switching stress, no need for a line-frequency transformer, lower voltage and current ratings for switching devices, and no harmonic distortion at the inverter output. Because of their versatility and usage of less switching components, cascaded H-Bridge Inverters (CHBMLI), Flying Capacitor Inverters (FCMLI), and Diode Clamped Inverters (DCMLI) are the three basic categories into which MLIs are categorized as presented by J. Rodriguez *et al.* [13].

In the literature Gupta N *et al.* [14] have presented the comprehensive review on the large scale grid integration of CHB-MLIs with PV integration and considered as the best of the three basic types of MLIs. In the MV to HV distribution industry, CHB-MLI-based SAPFs have become more and more well-liked for handling Power Quality (PQ) problems. Likewise, Singh A *et al.* [15] have put forth the control of 5-level DSTATCOM digitally implemented in the dSPACE -1104 board control by adaptive algorithms.

In addition to its function in harmonic correction, SAPF controls the movement of reactive power throughout the system to achieve a power factor of one at the grid connection. Mastromauro *et al.* [16] developed a single-phase, low-power photovoltaic system intended for harmonic compensation and grid voltage support. A decoupled adaptive noise detection-based control method for a four-leg VSC was proposed by Singh and Jain *et al.* in [17]. For tracking the reference signal, Gonzalez-Espín *et al.* [18] devised an adaptive controller based on the Schur-lattice IIR filter. A double-stage, three-phase, grid-integrated solar PV system was controlled using a fast zero-attracting normalised least mean forth algorithm by Singh *et al.* [19]. A sliding mode control and Lyapunov function-based method for maximum power tracking was published by Rezkallah *et al.* [20], integrating a DC-AC inverter to perform the functions of active power injection and harmonic correction in a solar PV grid-interfaced system.

A phase-locked loop (PLL) is the most common technology for handling various grid abnormalities in a power system, helping to synchronize the power converters with the grid. In addition, it is now widely used because its indirect measurement system detects deviations quickly, contributing to the frequency, voltage, and power control of the network, which are required to maintain power system stability.

Power converters use a variety of PLL technologies, each with a unique purpose and area of study. The compared PLLs have different features that meet the needs of different applications. Combining frequency-locked loops and second-order generalised integrators highlights how well the system handles frequency fluctuations, but it may also add complexity. Golestan. S *et al.* [21] *presented* as the Second-Order Generalised Integrator–Frequency-Locked Loop (SOGI-FLL). Similar to this, Second-Order Generalised Integrator PLL (SOGI-PLL) presented by Zhang, C *et al.* [22] uses second-order integrators to increase accuracy and rejection of distortion. Although it may be advanced, Ranjan. A *et al.* [23] put forth the Double Second-Order Generalised Integrator PLL (DSOGI-PLL) excels in distortion rejection, imbalance robustness, and precise positive sequence identification. Most widely used PLL is showcased by Liu, B *et al.* in [24] Synchronous Reference Frame PLL (SRF–PLL) could be subject to voltage distortions. Ortega. A *et al.* [25] have presented the Lag PLL (LAG-PLL)[25] main focus on phase accuracy, whereas noise reduction and simplicity are the main goals of Low-Pass Filter PLL (LPF-PLL)[26] and Moving Average Filter PLL (MAF-PLL) [27]. The integration of enhancements in Enhanced PLLs (E-PLL) [28] necessitates a thorough examination for application-specific suitability.

The traditional second-order generalised filter PLL (SOGI-PLL) [22] is quite well known and commonly applied, especially when grid conditions are distorted. However, it is widely acknowledged that when a DC offset in the input supply voltage is present, its performance suffers. To solve the issues the authors of [29] developed a modified notch filter second-order generalised integrator (MNFSOGI-PLL). When compared to traditional second-order filters, it is thought to offer better filtering capabilities. This study examines the multilevel inverter (MLI) control technique built on the MNFSOGI-PLL. The MLI controller was created with a dual focus. Its primary goal is to efficiently extract the main part of the load current. Second, it aims to assess the PLL's performance under various grid irregularities. The following is a list of the study's contributions:

1. Design and control of SAPF using 5-level CHB-MLI using phase-shifted PWM technique in closed loop operation.
2. Modelling of the proposed model in MATLAB/Simulink without/with PV interface.
3. Testing of simulation results with experimental model developed in the laboratory
4. Multifunctional capabilities of MNFSOGI are tested.
5. Comparison of the proposed filter with conventional schemes such as SRFT and SOGI filter

The organization of the paper is as follows. Section 2 describes the system configuration of the proposed filter along with the basic compensation principle of SAPF. Section 3 presents the modelling and analysis of MNFSOGI-PLL. The experimental performances under

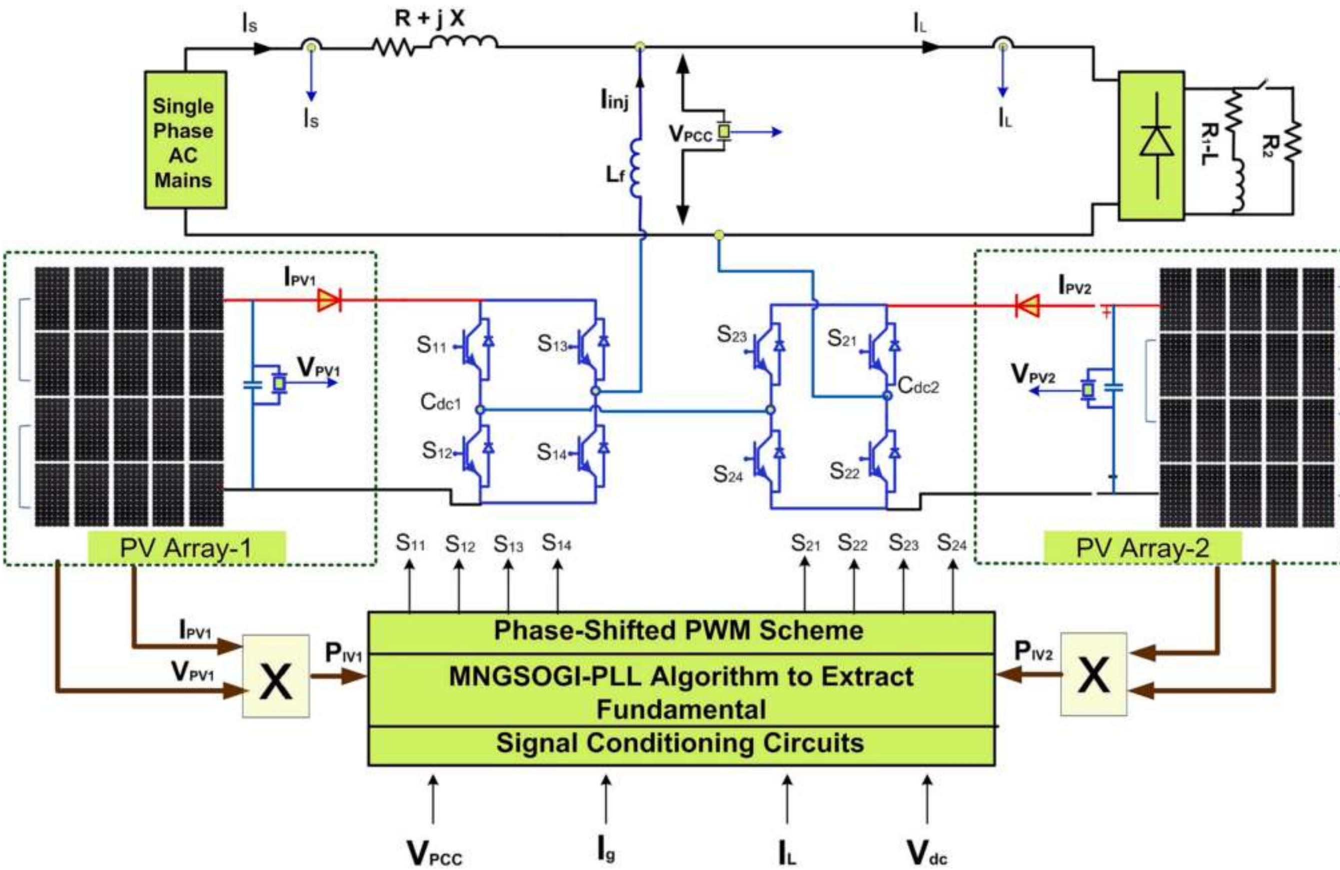

Fig. 1. Generalized block diagram of proposed system.

Table 1
Simulation Parameters.

S. No.	Parameter	Formula	Estimated Value	Used in Simulation
1.	DC link voltage	$E_{DC} = \sum_{j=1}^{N} E_{DC,j} = \frac{\sqrt{2} \times V_g}{m_i}$	172.82 V	200 V
2.	Interfacing Inductor	$L_{\inf} = \frac{E_{o,rms}}{8 \times g \times f_r \times \Delta I_g}$	3.05mH	3mH
3.	Grid Current	$I_g = \frac{P_{PV(\max)}}{V_g}$	18.18A	–
4.	SAPF Capacitors	$C_{DC,j} = \frac{P_{DCj}/E_{DCj}}{2 \times \omega_r \times E_{DC-ripple}}$	2560μF	2000μF

Where, $V_g = 110$ V (grid voltage), mi = 0.8(modulation index), Eo,rms = rms voltage, g = 0.5 (overloading factor), ripple in grid current$\Delta I_g = 1.8$A, DC link voltage and power is considered to be P_{DCj} and E_{DCj}.

distorted grid are explained in the Section 4. The comparative analysis of MNFSOGI-PLL and conventional PLL are presented in Section 5 and the concluding remarks are given in Section 6.

2. System configuration

Fig. 1 illustrates the schematic diagram of a single-phase 5-level CHB-MLI SAPF, depicting its connections to nonlinear loads and the single-phase AC grid. Key parameters like the voltage at the point of common coupling (PCC), load current (i_L), source current (i_s), and DC bus voltages (V_{DC1}, V_{DC2}) are monitored for controlling the SAPF's performance. An interface inductor (L_f) is strategically positioned to minimize AC output fluctuations and ripples. For generation of the necessary compensatory current that opposes the load current in the same phase, the SAPF unit employs the MNFSOGI method for current regulation. For the CHB-MLI to operate properly, it is essential to maintain both DC-link voltages in a steady state. A basic PI controller can effectively complete this duty.

First, the system undergoes an initial simulation using MATLAB/SIMULINK, followed by laboratory testing of a physical prototype model. In this proposed grid-tied PV array system with a single-phase, single-stage configuration; two PV arrays are connected to the DC-link side of the 5-level CHB-MLI. These PV arrays generate power during daytime, and the system seamlessly transitions to function as a SAPF unit at night, effectively managing harmonic compensation. The parameter values listed in Table 1.

The suggested system's closed-loop implementation is shown in Fig. 2. The suggested controller's main goals are divided into two categories:

1. To provide the AC grid with active power.
2. To achieve unity power factor operating on the supply side by reducing the harmonics caused by non-linear loads.

Maintaining stable DC link voltages is essential for the system to work effectively in both control modes. To achieve this, a proportional-integral (PI) controller is employed, and the error (DC) can be computed as indicated below.:

$$E_{DCe} = E_{DC-ref} - E_{DC} \tag{5}$$

The obtained error signal is fed to the PI controller, and Fig. 2 illustrates the calculation of I_{loss}. It can be expressed mathematically as follows:

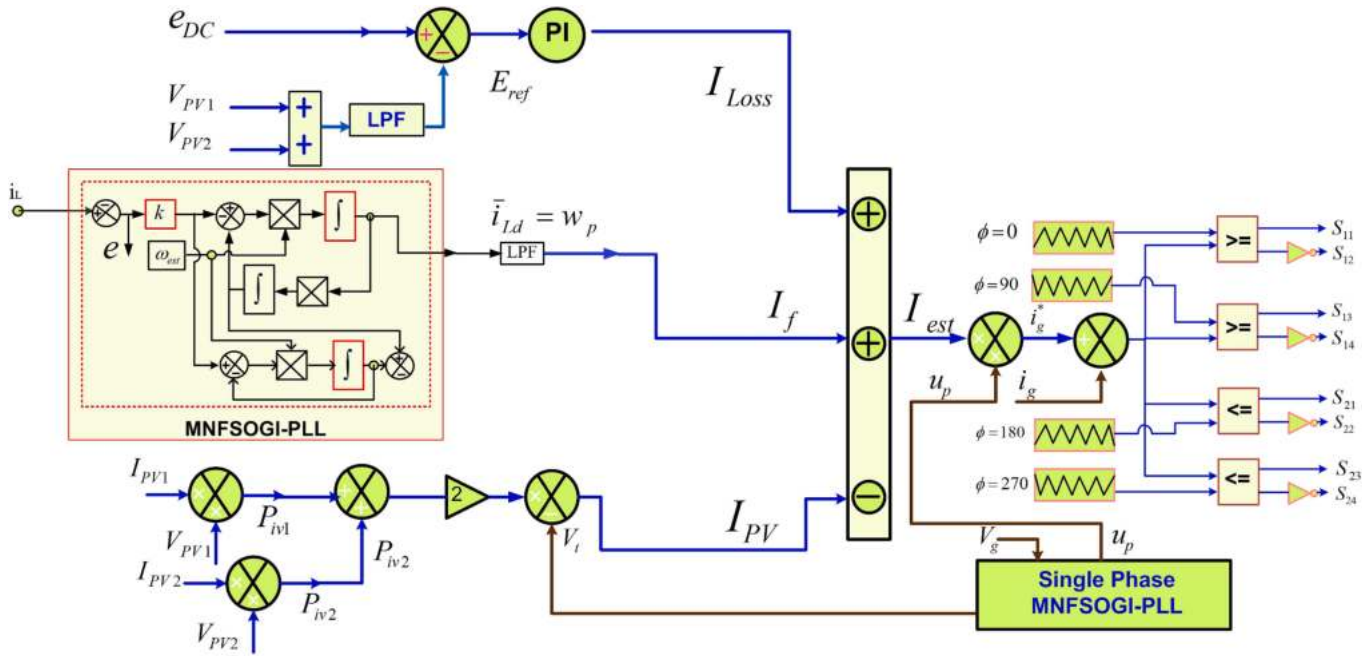

Fig. 2. Control Block Diagram of MNFSOGI-PLL.

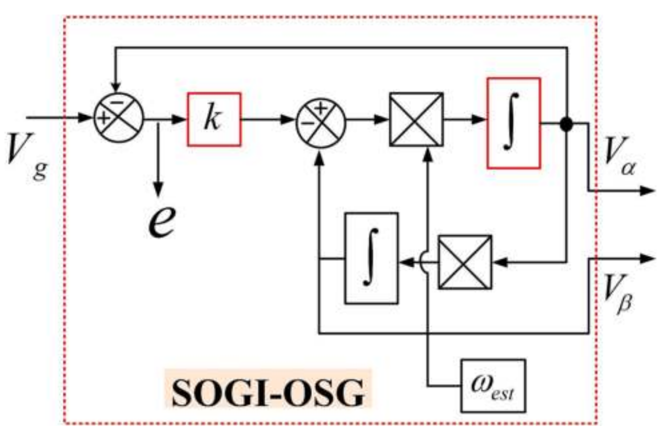

Fig. 3. Generalized structure of SOGI-PLL.

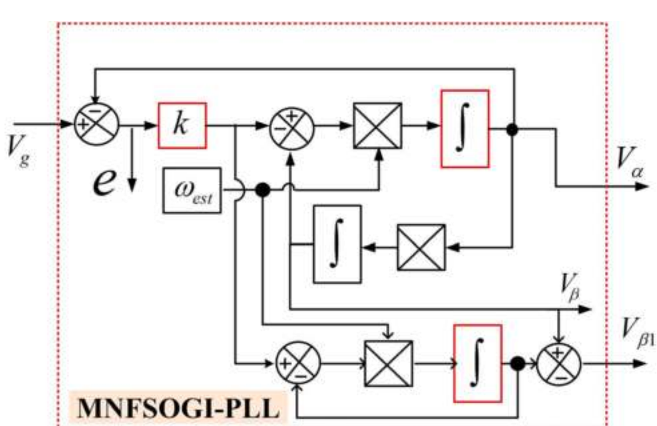

Fig. 4. Generalized block diagram of MNFSOGI-PLL.

$$I_{loss}(j+1) = I_{loss}(j) + k_p\{E_{DCe}(j+1) - E_{DCe}(j)\} + k_i E_{DCe}(j+1) \tag{6}$$

The feed forward term, denoted as I_{PV}, which is estimated using P_{PV1} & P_{PV2}, functions to handle the dynamics in the PV system represented as[15]

$$I_{PV} = \frac{2(P_{PV1} + P_{PV2})}{V_t} \tag{7}$$

The estimated load current, denoted as, is multiplied by the unit-synchronizing template (created by MNFSOGI-PLL) to get the reference current[15]

$$I_{est} = I_{loss} + I_f - I_{PV} \tag{9}$$

$$i_{gr}^* = u_p I_{est} \tag{8}$$

The SAPF generates firing pulses by subtracting the reference current from the grid current.

3. Performance of PV integrated single phase SAPF using MNFSOGI-PLL

Numerous grid anomalies have proliferated as a result of non-linear loads and the growing grid integration of a variety of renewable energy sources. These abnormalities include frequency fluctuations, phase shifts, voltage sags or swells, and DC offset. To guarantee the successful synchronisation of PV-integrated grid-connected systems, it is essential to precisely estimate phase, frequency, and voltage.

The Synchronous Reference Frame PLL (SRF-PLL) is a common method for unit template creation, but its poor tracking ability often leads to substantial total harmonic distortion (THD) in the grid current, especially in distorted grids. On the other hand, because of ability to handle a variety of grid anomalies well, orthogonal signal generator (OSG)-based PLLs, like the Park-PLL and Second-Order Generalised Integrator PLL (SOGI-PLL), have become more and more common. When it comes to monitoring grid-connected devices, especially when there are frequency changes, researchers and power engineers favour OSG-PLLs because they are more accurate and have stronger tracking capabilities than SRF-PLLs.

A major disadvantage of the SOGI-PLL is its incapacity to control DC-

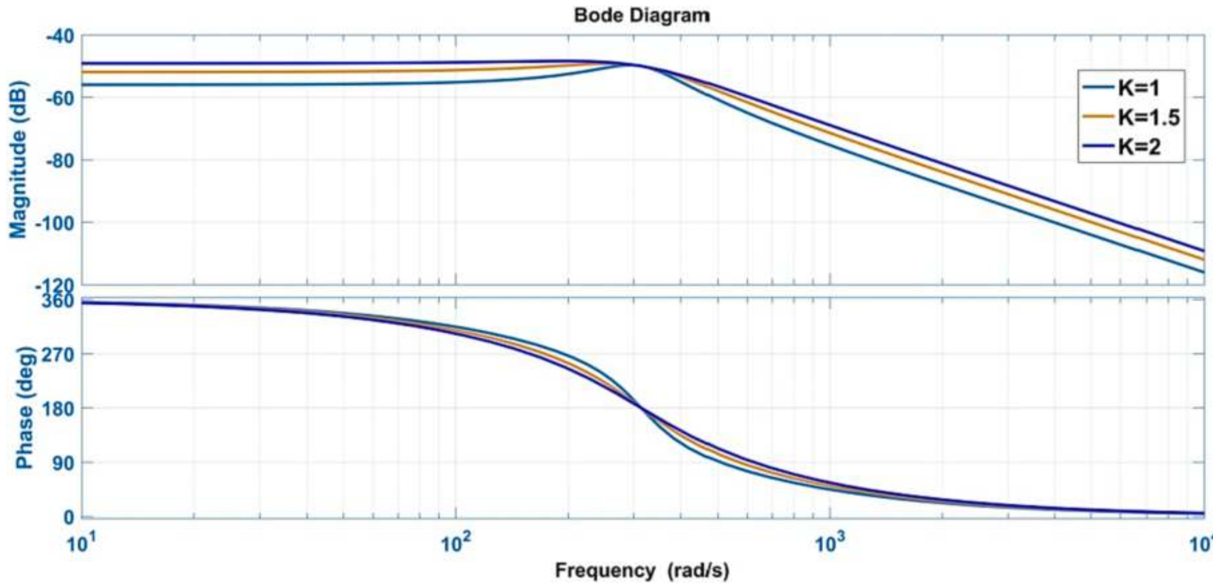

Fig. 5. Bode Plot analysis of MNFSOGI-PLL under varying gain parameter (K).

offset grid disturbances adequately. The issue results in a decline in the tracking capability of the SOGI-PLL when such disturbances occur, leading to considerable errors in phase and frequency estimates. A novel kind of PLL known as the Modified Notch Filter-Based SOGI-PLL (MNFSOGI-PLL) offers a solution to this issue. In addition to handling DC offset voltage, the MNFSOGI-PLL can reject inter-sub harmonics. The dynamic performance of the MNFSOGI-PLL has been evaluated in the presence of various grid anomalies, including phase shifts, DC offset, voltage sag/swell, and polluted grid conditions. The MNFSOGI-based controller has additionally enhanced the power quality (PQ) of a single-phase, single-stage grid-connected photovoltaic array system. It is utilised to extract the fundamental load current under both normal and distorted grid conditions, allowing the synthesis of grid reference current under non-linear loads. Fig. 3 illustrates the general structure of the conventional SOGI-PLL.

The Modified Notch Filter-SOGI-PLL (MNFSOGI), created expressly to overcome DC-offset issues, is seen in Fig. 4. The SOGI-PLL's quadrature output signal is most affected by DC offset. A transfer function is used to express the transfer function governing the quadrature signal from $V_{\beta 1}(s)$ to $V_g(s)$ given below[29]

$$T(s) = \frac{V_{\beta 1}}{V_g} \frac{k\,\omega_{eff}\, s(\omega_{eff} - s)}{(s + \omega_{eff})(s^2 + k\omega_{eff} s + \omega_{eff}^2)} \tag{10}$$

Further, the equation (10) can be simplied as[29]

$$T(s) = \frac{V_{\beta 1}}{V_g} \frac{(-k\,\omega_{eff})\, s^2 + k\omega_{eff}^2 s}{s^3 + (k\omega_{eff} + \omega_{eff})s^2 + (k\omega_{eff}^2 + \omega_{eff}^2)s + \omega_{eff}^3} \tag{11}$$

The MNFSOGI-PLL has a bandpass filter (BPF) property, which efficiently attenuates the grid's DC-offset elements, may be seen in the Bode plot diagram of the transfer function depicted in equation (11). However, making trade-offs involves choosing the right value for the constant gain (K). Fig. 5 shows the Bode plots produced at various gain K values. In the end, a value of 1.5 was selected for the suggested system because it provides a quick and dynamic response that can adjust to changes in load and solar irradiation. An integrator branch has been added to offset the DC offset component. A rapid dynamic reaction is seen when employing a high value of K, however the filtering ability is compromised.

The performance of the MNFSOGI-PLL in terms its behaviour and to plot its response characteristics, a pole-zero and Root locus plot have been shown in the Fig. 6(a-b). It has been seen that the poles are represented by ('x') and zeros are represented by ('o'). For a certain application, the location of poles and zeros plays can affect the frequency response, in the present case the system is found to be stable. In addition the root lies in the left half of the complex plane for all values of k, which means system is stable.

Now the performance of MNFSOGI-PLL is tested with differed grid distortions. In case-I, the grid is considered to have phase shift of $\pi/2$ from $t_1 = 0.1$ s to $t_2 = 0.2$ s and 20 % of DC offset is added in grid during $t_3 = 0.35$ s to $t_4 = 0.45$ s as shown in Fig. 7. The Figure shows that even under large step change in phase angle of 90° the MNFSOGI-PLL shows negligible peak to peak frequency overshoot and the undershoot is also observed to be very less. Negligible oscillations in peak to peak amplitude A_{vpp}(V) was observed. In addition during the case of 20 % DC –offset the oscillations observed in Δf and A_{vpp}(V) are negligible with the developed PLL.

In case-II, the grid is considered to have a voltage swell of 0.2 pu during $t_1 = 0.2$ s to $t_2 = 0.35$ s and distortion in grid voltage is considered during $t_3 = 0.35$ s to $t_4 = 0.45$ s as shown in Fig. 8. It is observed that under voltage swell also, tracking is fast and deviation in the peak to peak frequency estimation and also the peak to peak amplitude is small. It also takes just 1–2 cycles to reach steady state. Similar observations are recorded in the case of grid distortion. Moreover, the MNFSOGI-PLL correctly estimates the phase angle $\hat{\theta}$.

3.1. Simulation results with Single-Phase single stage PV array based MNFSOGI controller under normal and distorted grid conditions

Fig. 9 shows the simulation results for a number of parameters, including the total DC link voltage (V_{DC}), load current (i_L), grid voltage (V_g), and grid current (i_g), all derived with the MNFSOGI-PLL. Various solar radiation levels and dynamic load variations that occur between t=0.3s and 0.5s and t=0.5s and 0.7s, are taken into account while showcasing these results. Notably, the PV arrays inject active power into the grid, resulting in the phase-shift of the grid current with respect to the grid voltage seen in the picture. It is crucial to note that a little variation in the overall DC link voltages can be seen even as solar energy decreases from 1000W/m^2 to 600W/m^2.

Now, the MNFSOGI controller's performance is evaluated with a distorted grid. The model is simulated in MATLAB/Simulink and the grid is purposefully contaminated by adding an odd number of harmonics. In more detail, the grid is regarded as normal from 0.2 s to t

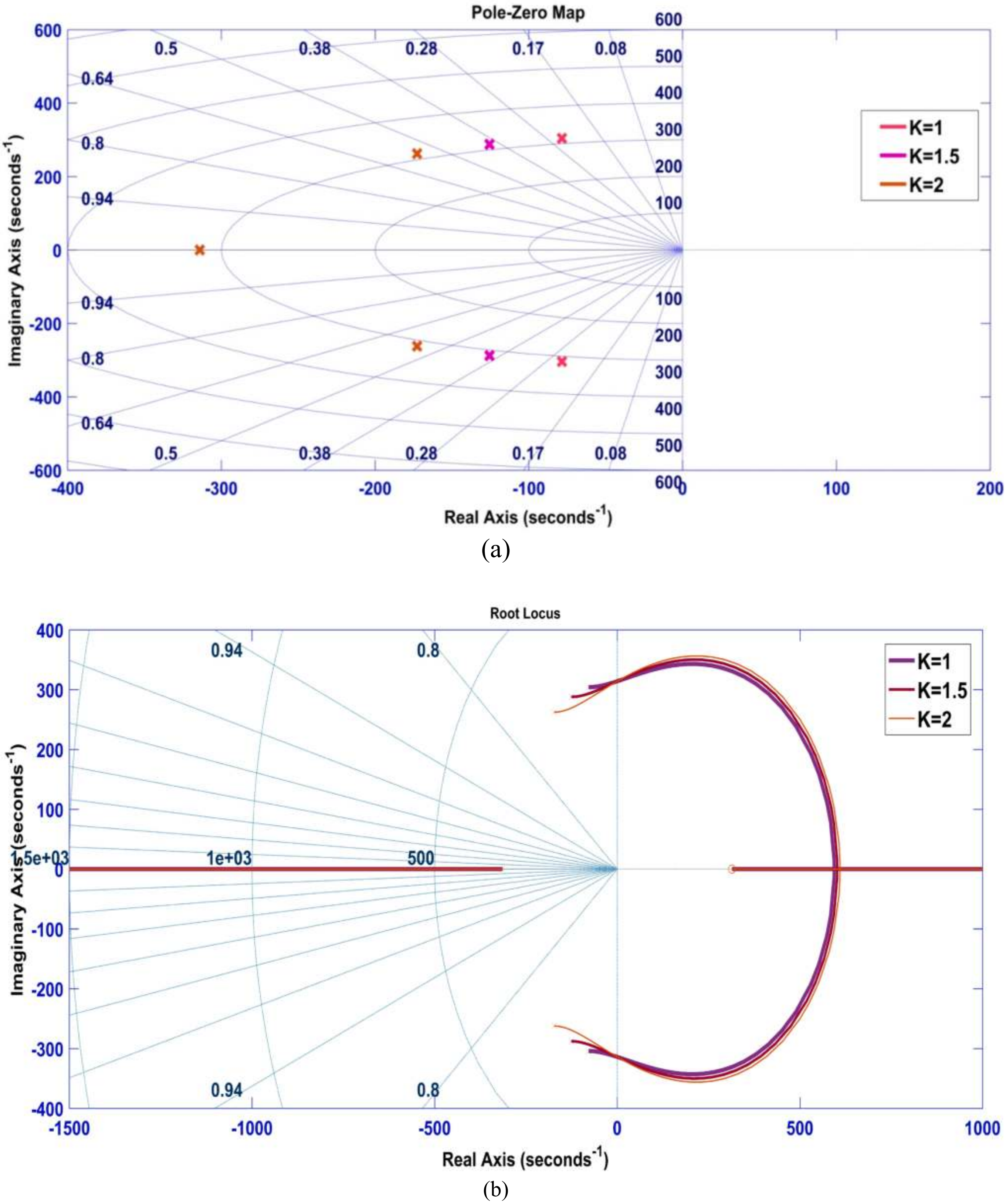

Fig. 6. (a) Pole-Zero plot analysis (b) Root locus analysis of MNFSOGI-PLLL.

seconds, but after t = 0.6 s, it becomes polluted, as seen in Fig. 10. Additionally, the solar irradiation is changed, starting at 1000 W/m^2 at t = 0.3 s, dropping to 600 W/m^2, and then increasing to 1000 W/m^2 at t = 0.5 s. The grid current displays sinusoidal behaviour but remains out of phase with the grid voltage during the decrease in solar irradiation, which takes place from 0.3 s $\leq$ t $\leq$ 0.5 s.

Fig. 11(a-e) depict the %THD performance of the MNFSOGI-controller under normal and distorted grid conditions.

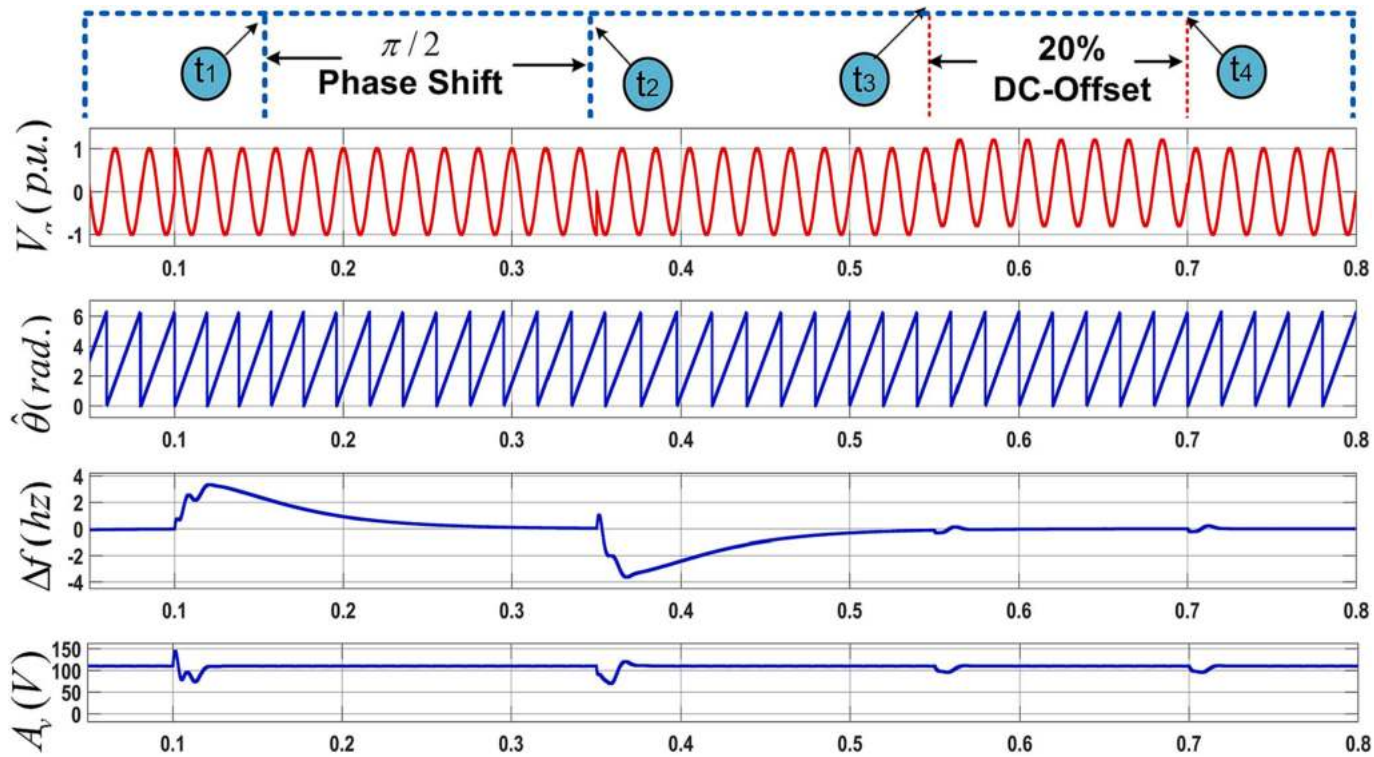

Fig. 7. Simulation performance of SOGI-PLL under phase shift and 20% DC – Offset.

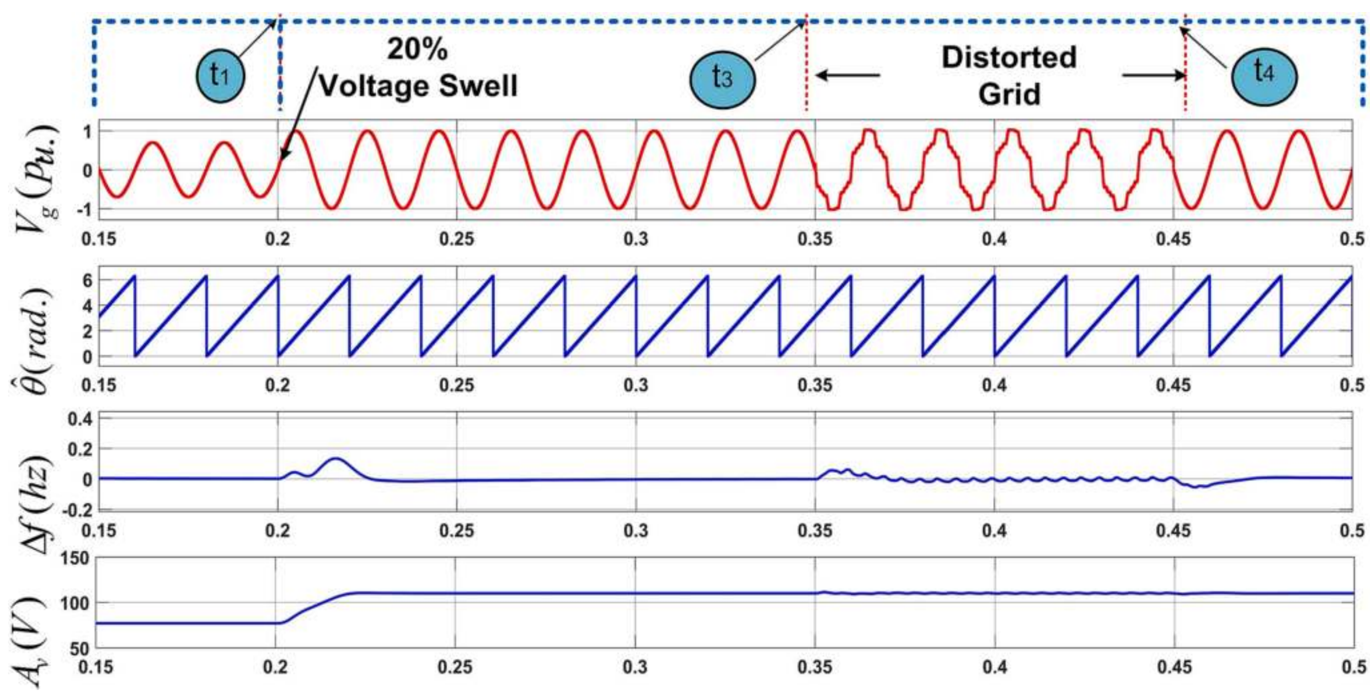

Fig. 8. Simulation performance of MNFSOGI-PLL under 20% voltage sag and distorted grid.

Fig. 11(a-b) shows the waveforms of grid voltage with THD of 0.03 % in normal and 24.75 % in distorted grid. The load current THD of 26.85 % and 36.00 % was found before compensation followed by source current has same THD before compensation as shown in Fig. 11(c-d). But, after compensation, the THD of source current was found to be 1.50 % under normal and 3.96 % in distortion as depicted in Fig. 11(e-f). The obtained THD values are safely below the 5 % cap imposed by IEEE-1547 guidelines. Even in the presence of varying solar irradiation and a contaminated grid, the MNFSOGI-controller's performance continuously stays adequate.

4. Experimental results and discussion

The OP-4512 model of the OPAL-RT system was utilised to experimentally validate the results of an extensive simulation of the proposed system performed in the MATLAB-Simulink environment. Fig. 12 shows

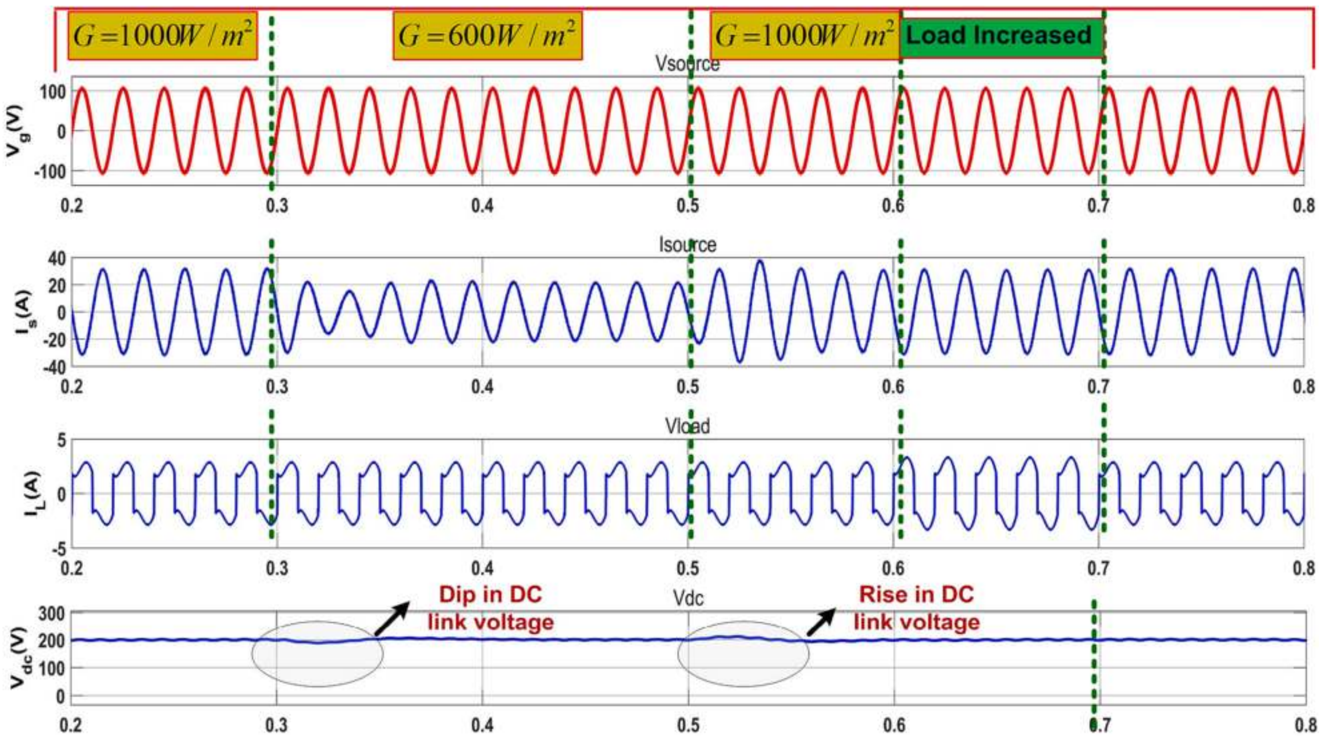

Fig. 9. Simulation results with varying load and solar irradiance.

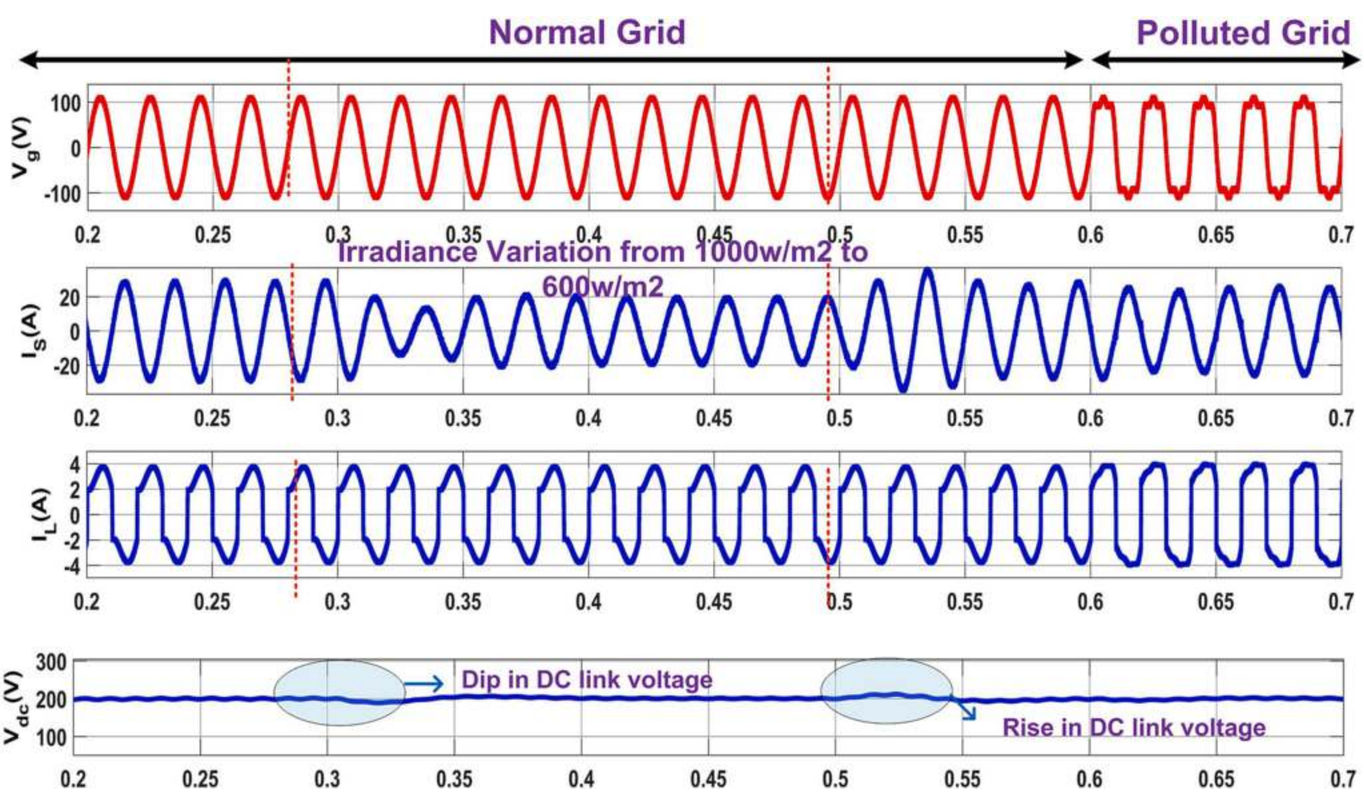

Fig. 10. Simulations results of single stage single phase PV array grid connected system under distorted grid conditions.

the physical prototype model that was used as a guide during the experimental validation procedure. The MATLAB simulation results were extensively validated using the OPAL-RT controller-based Hardware-in-Loop (HIL) system. The adaptability of the system is supported by the MNF-SOGI control method, which is the result of the effective interaction between OPAL-RT and MATLAB/Simulink.

Most importantly, the HIL platform and the RT-Lab simulation environment are essential parts of the OPAL-RT system. Notable is the addition of the FPGA processor, which is well known for its quick signal processing capability and improves the OPAL-RT engine's overall

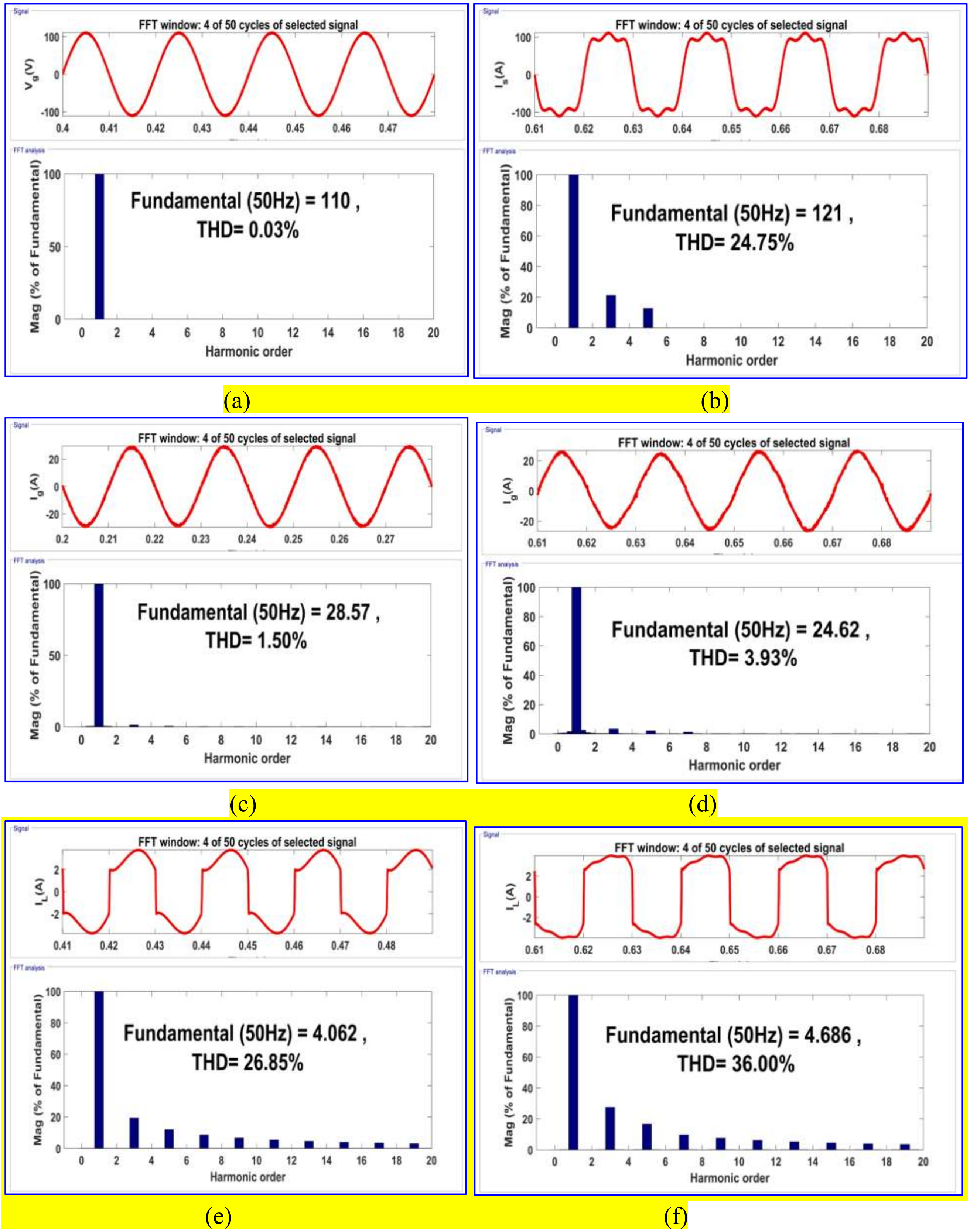

Fig. 11. Case I(a-c): THD(%) performance of Vg(V) under normal and distorted grid Case II(c-d) THD(%) performance of ig(A) under normal and distorted grid Case III(e-f): THD(%)performance of iL(A) under polluted grid conditions.

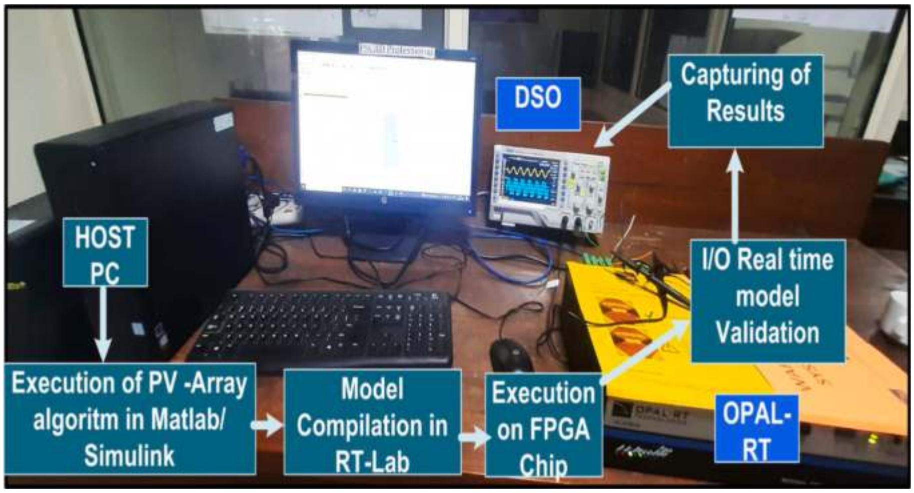

Fig. 12. Experimental implementation of proposed algorithm on OPAL-RT.

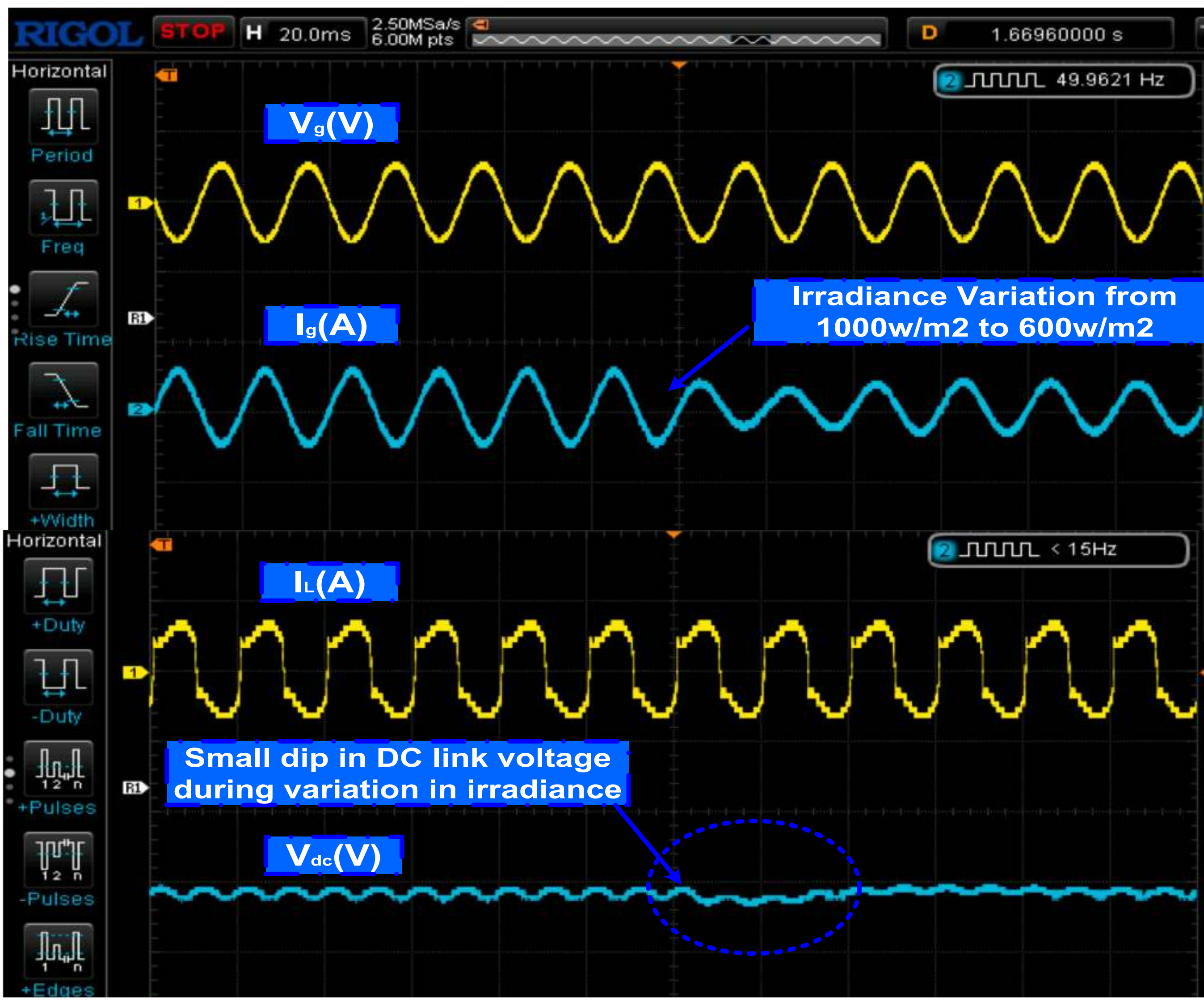

(a)

Fig. 13. Experimental Results (a) Grid parameters (b) Solar PV Array parameters.

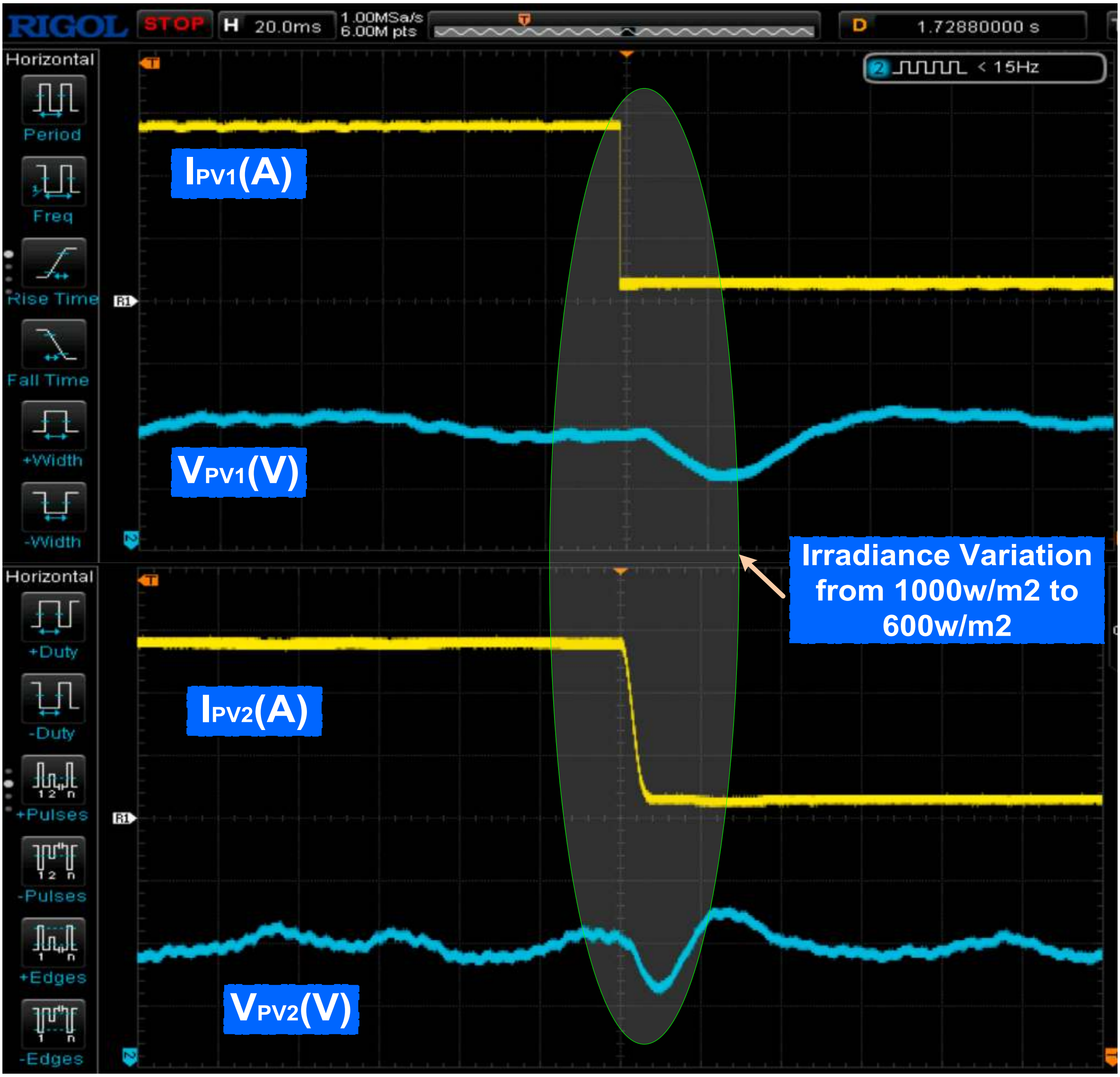

(b)

Fig. 13. (*continued*).

performance. This integration guarantees a smooth transition from simulation to real-world validation, which enhances the suggested system's dependability and efficacy.

Fig. 13(a, b) shows the experimental results produced from OPAL-RT. The grid voltage (v_g), grid current (i_g), total DC link voltage (V_{dc}), and load current (i_L) are shown in Fig. 13(a) as the solar irradiation varies from 1000 W/m^2 to 600 W/m^2. It is noteworthy to note that the DC link voltage quickly stabilises at 200 V in just 1 ~ 2 cycles cycles as solar irradiation varies. Although there are non-linear loads at the point of common coupling (PCC), the grid current behaves sinusoidally and maintains a small phase difference, keeping the grid connection's power factor close to one.

The solar irradiance is varied from 1000 W/m^2 to 600 W/m^2 and its effect is observed on parameters viz PV array-1 output voltage V_{PV1}(V), PV array-2 output voltage V_{PV2}(V), PV-1 and PV-2output current I_{pv1} and I_{pv2} as shown in Fig. 13(b).

Experimental testing with a malformed grid has now been conducted on the single-stage grid-connected system. The experimental results achieved under these grid pollution conditions are shown in Fig. 14. In the setting of a distorted grid environment, the findings for fluctuations in solar irradiance—from 1000 W/m^2 to 600 W/m^2 and back to 1000 W/m^2—are shown in the Figure. The outcomes show that the grid current keeps its sinusoidal properties while continuing to be out of phase with the grid voltage. Notably, the system's performance is judged to be good in these contaminated grid conditions. The grid current's Total Harmonic Distortion (THD), which is below 5 %, complies with IEEE-1547 requirements for PV integration. Additionally, Fig. 15 illustrates the empirically observed power flow inside the system under these

Fig. 14. Processor-in-loop results of vg(V) & ig(A) under varying solar irradiance and polluted grid conditions.

contaminated grid conditions. It has been noted that the active and reactive power flows adapt as irradiance levels change.

5. Comparative performance of PLL algorithms for single phase PV integrated grid connected system

The comparative performance based on frequency and amplitude tracking abilities of three different PLLs—the E-PLL,DSOGI-PLL, MAF-PLL and MNFSOGI-PLL—are examined and presented in this section. In assessing the performance of various phase-locked loop (PLL) techniques under different power quality disturbances, namely voltage sag of 20 %, DC-offset of 20 %, phase shift of $\pi/2$, and harmonics in the grid, distinct characteristics emerge for each PLL. Fig. 16a and Fig. 16b exhibits the performance of various PLLs in frequency Variation of E-PLL, DSOGI-PLL, MAF-PLL and MNFSOGI-PLL under phase shift and DC Offset Conditions and amplitude variations are presented in Fig. 17a and Fig. 17b.

The E-PLL and DSOGI-PLL exhibit moderate performance in handling a voltage sag of 20 %, with both methods demonstrating satisfactory outcomes in addressing harmonics in the grid. However, their effectiveness diminishes in the presence of a 20 % DC-offset.

On the other hand, the MAF-PLL proves to be robust in mitigating

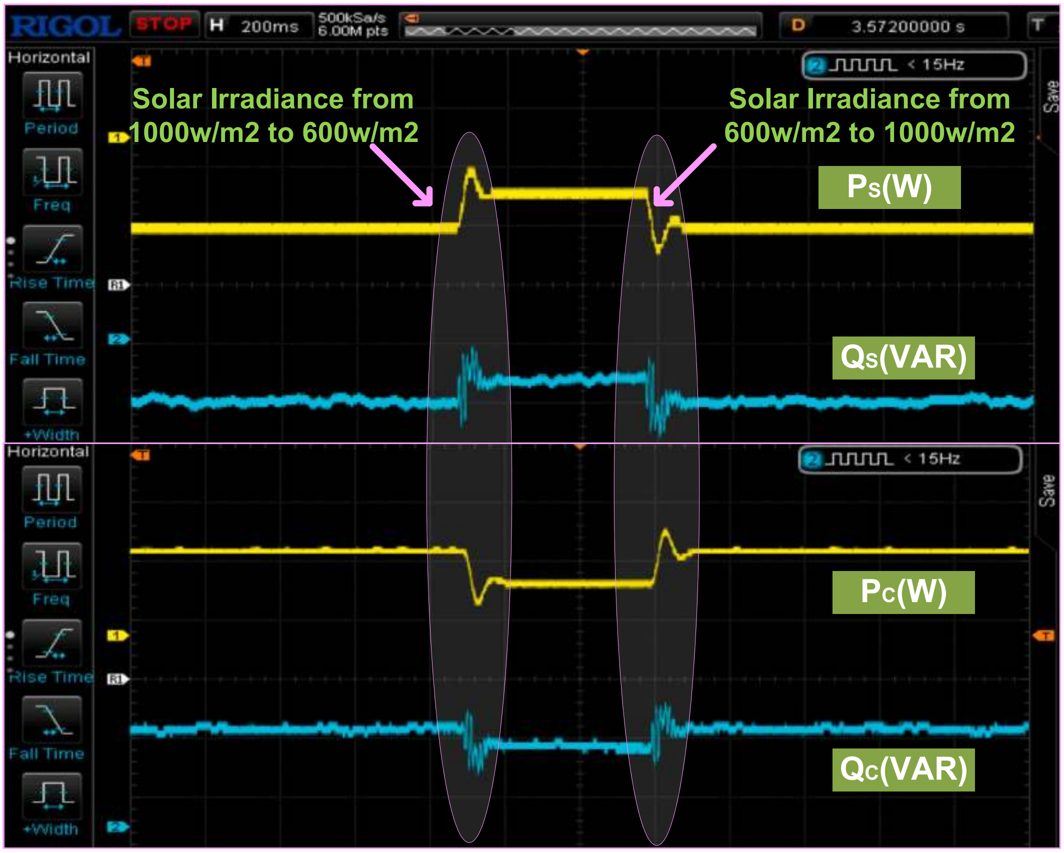

Fig. 15. Processor-in-loop results of power flow in the proposed system.

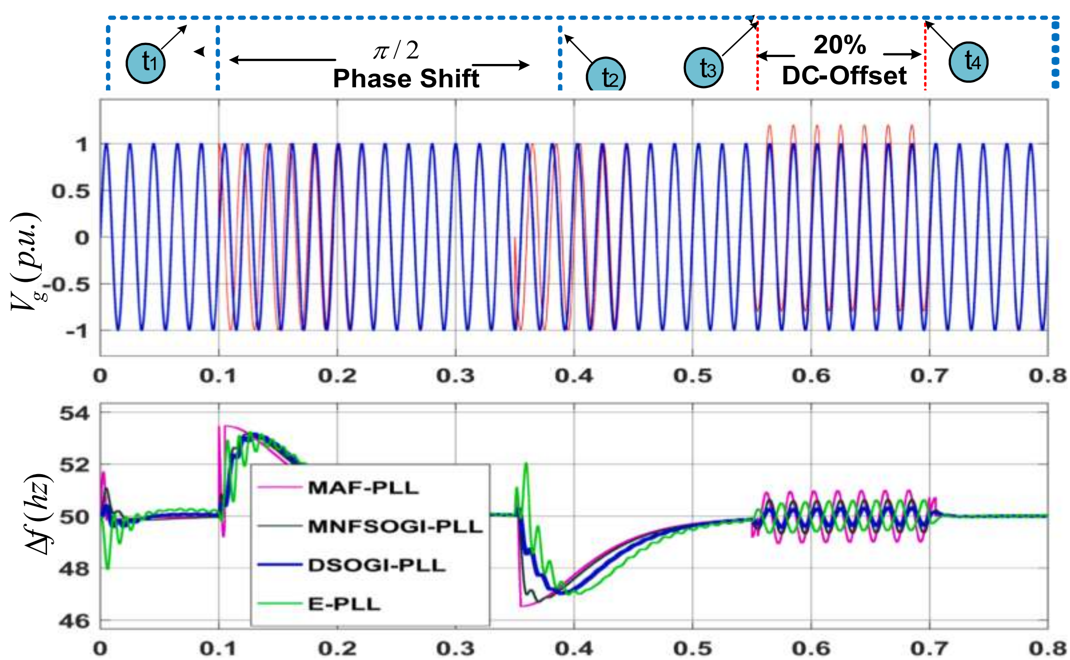

Fig. 16a. Frequency Variation of E-PLL, DSOGI-PLL, MAF-PLL and MNFSOGI-PLL under phase shift and DC Offset Conditions.

voltage sags, shows good performance. Yet, it falls short in performance on handling DC-offsets. The MFSOGI-PLL stands out as the most versatile, achieving the best performance across all disturbances. It excels in addressing voltage sag, DC-offset, phase shift and harmonics as tabulated in Table 1. In summary, the MFSOGI-PLL emerges as the most comprehensive solution, providing superior performance across a range of power quality challenges (see in Table 2).

Important insights into the various performances of E-PLL, DSOGI-PLL, MAF-PLL, and MNFSOGI-PLL can be obtained by a comparative study of their properties. First, in terms of convergence, MNFSOGI-PLL is

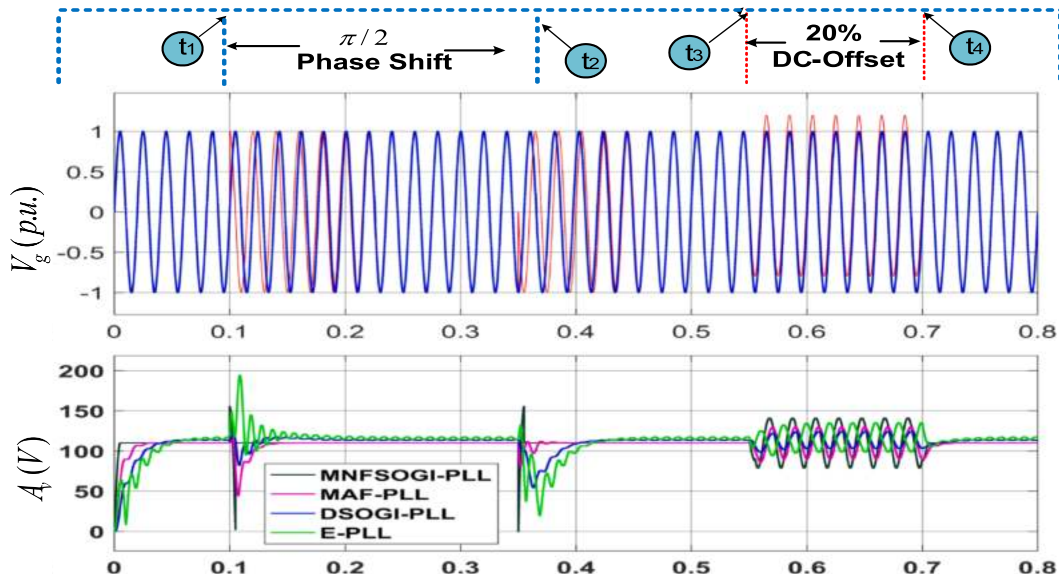

Fig. 16b. Amplitude Variation of E-PLL, DSOGI-PLL, MAF-PLL and MNFSOGI-PLL under phase shift and DC Offset Conditions.

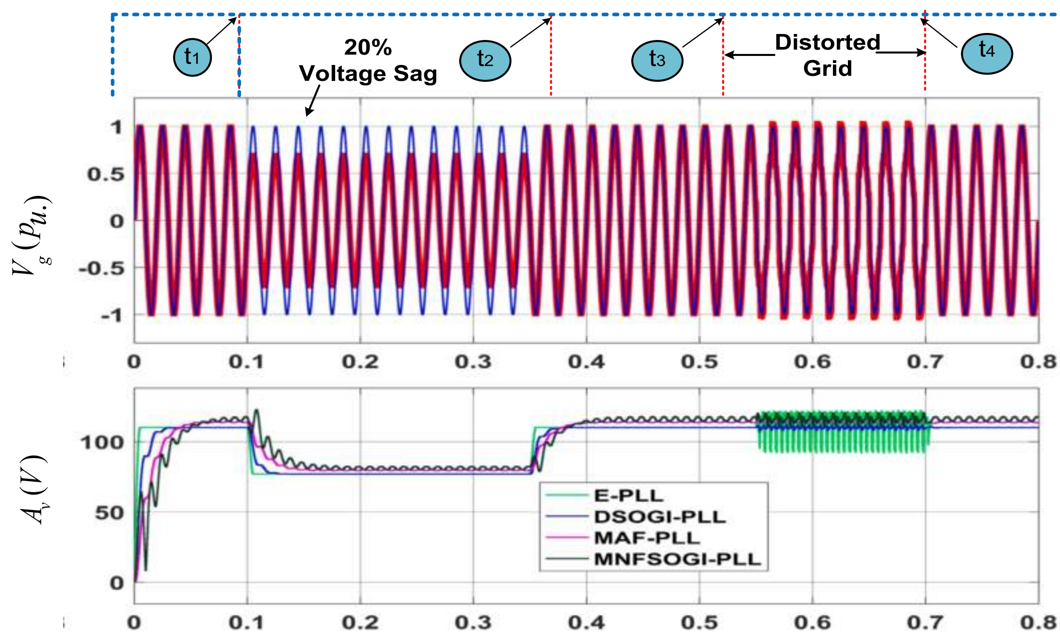

Fig. 17a. Frequency Variation of E-PLL, DSOGI-PLL, MAF-PLL and MNFSOGI-PLL under voltage sag and distorted grid conditions.

the fastest, taking only 1–2 cycles to reach convergence, while E-PLL, DSOGI-PLL, and MAF-PLL all took longer (2–3, 3–4, and 3–4 cycles, respectively). MNFSOGI-PLL exhibits improved stability as evidenced by the much lower presence of oscillations in fundamental weights when compared to other approaches. MNFSOGI-PLL has exceptional performance in a simulation research that looks at the Total Harmonic Distortion (THD) of current, having the lowest THD for both supply and load currents as tabulated in Table 3.

Additionally, when compared to E-PLL, DSOGI-PLL, and MAF-PLL, MNFSOGI-PLL shows a more moderate error level. In terms of DC link voltage oscillations, MNFSOGI-PLL performs better than E-PLL, DSOGI-PLL, and MAF-PLL (5–6 V, 3–5 V, and 3–4 V, respectively), with the narrowest amplitude range (1–2 V). Last but not least, MNFSOGI-PLL outperforms E-PLL, DSOGI-PLL, and MAF-PLL (70 µs, 55 µs, and 60 µs, respectively) in terms of real-time processing capabilities thanks to its 50 µs sampling time. MNFSOGI-PLL shows promise as a solution, outperforming the other PLL techniques in terms of faster convergence, less oscillations, better harmonic performance, and increased stability.

6. Conclusion

This research concludes by providing a thorough investigation of an improved control strategy for grid-connected single-phase photovoltaic systems. The approach focuses on a five-level cascaded multilevel inverter (MLI) that serves as an active filter. The system has two distinct modes of operation: it can be used to address harmonics and improve the power factor by injecting active power during the day and acting as a Shunt Active Power Filter (SAPF) at night. When used as a PLL, the Modified Notch Filter Second Order Generalised Integrator (MNFSOGI) scheme is essential for estimating the basic component of non-linear load current.

The results of the research highlight how much better the suggested

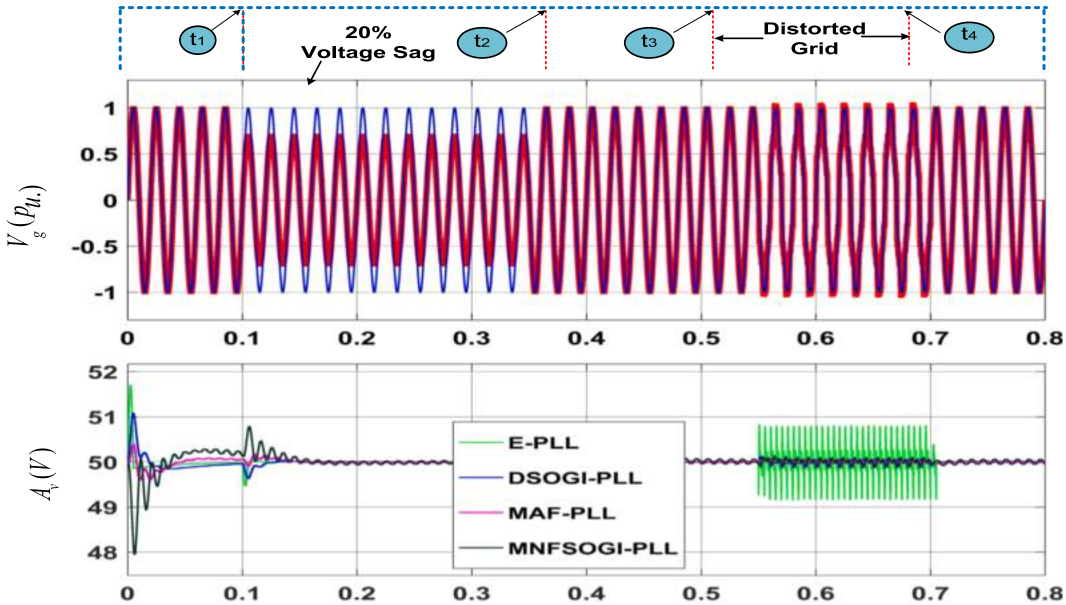

Fig. 17b. Amplitude Variation of E-PLL, DSOGI-PLL, MAF-PLL and MNFSOGI-PLL under voltage sag and distorted grid conditions.

Table 2
Performance comparison table of various-PLL under grid abnormalities.

Cases	E-PLL	DSOGI-PLL	MAF-PLL	MFSOGI-PLL
Voltage Sag of 20 %	Moderate	Moderate	Good	Best
DC-offset of 20 %	Unsatisfactory	Unsatisfactory	Moderate	Satisfactory
Phase Shift of $\pi/2$	Unsatisfactory	Moderate	Moderate	Satisfactory
Harmonics in Grid	Satisfactory	Satisfactory	Good	Good

MNFSOGI controller can handle various kinds of grid anomalies than other techniques like the E-PLL, DSOGI-PLL and MAF-PLL. Interestingly, the MNFSOGI controller demonstrates exceptional efficacy in resolving Power Quality (PQ) concerns in both normal and distorted grid condition test cases, such as 20 % voltage sag, 20 % DC offset, 20 % phase shift, and harmonics in the grid.The validation process involved a synergy of simulation and experimental results, conducted rigorously through the OPAL-RT real-time data simulator and MATLAB/Simulink software. The successful implementation of the proposed system positions the MNFSOGI controller as a robust and reliable solution for controlling multilevel inverters in scenarios involving distorted grid conditions.

Future directions for single-phase grid-connected PV systems involve advanced control strategies, including AI and adaptive techniques for optimized performance. Dynamic adaptive modes for real-time adjustments and considerations for energy storage integration and industry standards are crucial for future research.

CRediT authorship contribution statement

Praveen Bansal: Conceptualization, Methodology, Software, Validation, Formal analysis, Investigation, Resources, Data curation, Writing – original draft, Writing – review & editing, Visualization. **Shishir Dixit:** Conceptualization, Methodology, Software, Validation, Formal analysis, Investigation, Resources, Visualization. **Saket Gupta:** Conceptualization, Methodology, Software, Validation, Formal analysis, Investigation, Resources, Data curation, Writing – review & editing. **Majed A. Alotaibi:** Conceptualization, Methodology, Software, Validation, Formal analysis, Investigation, Resources, Data curation, Writing – original draft, Writing – review & editing, Visualization, Supervision, Project administration, Funding acquisition. **Hasmat Malik:** Conceptualization, Methodology, Software, Validation, Formal analysis, Investigation, Resources, Data curation, Writing – original draft, Writing – review & editing, Visualization, Supervision, Project administration, Funding acquisition. **Fausto Pedro García Márquez:** Conceptualization, Methodology, Software, Validation, Formal analysis, Investigation, Resources, Data curation, Writing – original draft, Writing – review & editing, Visualization, Supervision.

Funding

The authors extend their appreciation to the Researchers Supporting Project at King Saud University, Riyadh, Saudi Arabia, for funding this research work through the project number RSP2023R278.

Table 3
Comparison of Various PLL Techniques.

S.No.	Features		E-PLL	DSOGI-PLL	MAF-PLL	MNFSOGI-PLL
1.	Convergence		Slower (2 ~ 3 cycles)	Slower (3 ~ 4 cycles)	Slower (3 ~ 4 cycles)	**Faster (1 ~ 2 cycles)**
2.	Oscillations in fundamental weights		More	Less	Less	Very less
3.	THD of current	Supply current	3.92 %	4.21 %	3.57 %	**1.50 %**
4.	(Simulation study)	Load current	26.85 %	26.85 %	26.85 %	26.85 %
5.	Error		More	Moderate	Moderate	Moderate
6.	DC link Voltage Oscillations		5–6 V	3–5 V	3–4 V	1–2 V
7.	Sampling time		70 µs	60 µs	60 µs	50 µs

Declaration of competing interest

The authors declare that they have no known competing financial interests or personal relationships that could have appeared to influence the work reported in this paper.

Acknowledgement

The authors extend their appreciation to the Researchers Supporting Project at King Saud University, Riyadh, Saudi Arabia, for funding this research work through the project number RSP- 2021/278. The authors would like to acknowledge the support from Intelligent Prognostic Private Limited Delhi, India Researcher's Supporting Project.

The authors would like to acknowledge the research support from Universiti Teknologi Malaysia (UTM) through UTM Fundamental Research Grant (UTMFR), code Q.J130000.3823.23H05.

The Authors are thankful to Madhav Institute of Technology and Science, Gwalior, Madhya Pradesh, India for carry out experimental work on OPAL-RL (Model No.4510) Real Time Simulator in the Power System lab of Electrical Engineering Department.

Appendix

V_g/V_s, Grid/source voltage; i_g/i_s, Grid/source current; i_L, Load current; i_c, Compensating current; $E_{dc\text{-}ref}$, Reference DC link voltage; V_{dc1}, DC link voltage across capacitor-1; V_{dc2}, DC link voltage across capacitor-2; E_{dc}, DC link voltage; L_{inf}, Interfacing Inductor; f_{sw}, Switching Frequency; ΔI_{cr-pp}, Peak to Peak ripple current; I_{PV1}, I_{PV2}, Current of PV–arrays; V_{PV1}, V_{PV2}, Voltage of PV–arrays; m, Number of voltage levels; m_f, Modulation index; i_s, Source current; i_s*, Reference supply current; f_{cr}, Carrier frequency; f_m, Modulating Frequency; I_{Loss}, DC loss component; K_d, Proportional gain; K_i, Integral gain; I_f, Fundamental component of load current; I_{eff}, Effective average weight; u_p, Unit vector template; θ, Actual phase angle; $\widehat{\theta}$, Estimated phase angle; ω_{eff}, normal grid frequency; $\widehat{\omega}$, estimated frequency; A_{vpp}, amplitude of grid voltage; Δf, Difference between estimated and actual frequency; CHB, cascaded H-Bridge; PWM, pulse width modulation; PLL, Phase lock loop.

References

[1] Agarwal RK, Hussain I, Singh B. Dual-function PV-ECS integrated to 3P4W distribution grid using 3M-PLL control for active power transfer and power quality improvement. IET Renew Power Gener 2018;12(8):920–97. https://doi.org/10.1002/9781119710905.ch12.

[2] Md Alamgir Hossain, Hemanshu Roy Pota, Md Jahangir Hossain, Frede Blaabjerg, Evolution of microgrids with converter-interfaced generations: Challenges and opportunities. Int J Electr Power Energy Syst, Volume 109,2019, pp.160-186,. 10.1016/j.ijepes.2019.01.038.

[3] IEEE Application Guide for IEEE Std. 1547, IEEE standard for interconnecting distributed resources with electric power systems, IEEE Std. 1547.2–2008, 2009. 10.1109/IEEESTD.2008.4816078.

[4] Kirmani S, Jamil M, Akhtar I. Economic feasibility of hybrid energy generation with reduced carbon emission. IET Renew Power Gener 2018;12(8):934–42. https://doi.org/10.1049/iet-rpg.2017.0288.

[5] Mejdar RS, Salimi M, Zakipour A. Design and implementation of a low cost grid-connected 5 kVA photovoltaic system with load compensation capability. J Power Electron 2016;16(6):2306–14. https://doi.org/10.6113/JPE.2016.16.6.2306.

[6] Asiminoael L, Blaabjerg F, Hansen S. Detection is key-harmonic detection methods for active power filter applications. IEEE Ind Appl Mag 2007;13(4):22–33. https://doi.org/10.1109/MIA.2007.4283506.

[7] Lin X-M, Natalia Kireeva AV, Timoshin AN, Abdul-Malek Z, Kamyab H. A multi-criteria framework for designing of stand-alone and grid-connected photovoltaic, wind, battery clean energy system considering reliability and economic assessment. Energy 2021;224. https://doi.org/10.1016/j.energy.2021.120154.

[8] Nasri S, Zamanifar M, Naderipour A, et al. Stability and dynamic analysis of a grid-connected environmentally friendly photovoltaic energy system. Environ Sci Pollut Res 2023;30:71701–13. https://doi.org/10.1007/s11356-021-15255-w.

[9] Amirreza Naderipour, Hesam Kamyab, Jiří Jaromír Klemeš, Reza Ebrahimi, Shreeshiva dasan Chelliapan, Saber Arabi Nowdeh, et al., Optimal design of hybrid grid-connected photovoltaic/wind/battery sustainable energy system improving reliability, cost and emission, Energy, Volume 257, 2022. 10.1016/j.energy.2022.124679.

[10] Naderipour A, Abdul-Malek Z, Nasri S, Arabi Nowdeh S, Kamyab H, Chelliapan S, et al. Novel designing framework of stand-alone and grid-connected hybrid photovoltaic/wind/battery renewable energy system considering reliability, cost and emission indices. Chem Eng Trans 2021;83:565–70. https://doi.org/10.3303/CET2183095.

[11] Singh B, Al-Haddad K, Chandra A. A review of active filters for power quality improvement. IEEE Trans Ind Electron 1999;46(5):960–71. https://doi.org/10.1109/41.793345.

[12] Mahela OP, Shaik AG, Gupta N. A critical review of detection and classification of power quality events. Renew Sust Energy Rev 2015;41:495–505. https://doi.org/10.1016/j.rser.2014.08.070.

[13] Franquelo LG, Rodriguez J, Leon JI, Kouro S, Portillo R, Prats MAM. The age of multilevel converters arrives. IEEE Ind Electron Mag 2008;2(2):28–39. https://doi.org/10.1109/MIE.2008.923519.

[14] Ray S, Gupta N, Gupta RA. A comprehensive review on cascaded H-bridge inverter-based large-scale grid-connected photovoltaic. IETE Tech Rev 2017;Aug;34:463–77. https://doi.org/10.1080/02564602.2016.1202792.

[15] Bansal P, Singh A. Nonlinear adaptive normalized least mean absolute third algorithm for the control of five-level distribution static compensator. Int J Circ Theor Appl 2021;49(9):2840–64. https://doi.org/10.1002/cta.3045.

[16] Mastromauro RA, Liserre M, Dell'Aquila A. Single-phase grid-connected photovoltaic systems with power quality conditioner functionality. European Conference on Power Electronics and Applications, Aalborg, Denmark 2007;2007:1–11. https://doi.org/10.1109/EPE.2007.4417672.

[17] Singh B, Jain C. A decoupled adaptive noise detection based control approach for a grid supportive SPV system. IEEE Trans Ind Appl 2017;53(5):4894–902. https://doi.org/10.1109/TIA.2017.2723341.

[18] Gonzalez-Espin F, Patrao I, Figueres E, Garcera G. An adaptive digital control technique for improved performance of grid connected inverters. IEEE Trans Ind Inf 2013;9(2):708–18. https://doi.org/10.1109/TII.2012.2225437.

[19] Singh AK, Hussain I, Singh B. Double-stage three-phase grid integrated solar PV system with fast zero attracting normalized least mean fourth based adaptive control. IEEE Trans Ind Electron 2018;65(5):3921–31. https://doi.org/10.1109/TIE.2017.2758750.

[20] Rezkallah M, Sharma SK, Chandra A, Singh B, Rousse DR. Lyapunov function and sliding mode control approach for the solar PV grid interface system. IEEE Trans Ind Electron Jan. 2017;64(1):785–95. https://doi.org/10.1109/TIE.2016.2607162.

[21] Golestan S, Guerrero JM, Vasquez JC, Abusorrah AM, Al-Turki Y. Standard SOGI-FLL and Its Close Variants: Precise Modeling in LTP Framework and Determining Stability Region/Robustness Metric. IEEE Trans Power Electron 2021;36:409–22. https://doi.org/10.1109/TPEL.2020.2997603.

[22] Zhang C, Foyen S, Suul JA, Molinas M. Modeling and Analysis of SOGI-PLL/FLL-Based Synchronization Units: Stability Impacts of Different Frequency-Feedback Paths. IEEE Trans Energy Convers 2021;36:2047–58. https://doi.org/10.1109/TEC.2020.3041797.

[23] Ranjan A, Kewat S, Singh B. DSOGI-PLL with in-loop filter based solar grid interfaced system for alleviating power quality problems. IEEE Trans Ind 2021;57:730–40. https://doi.org/10.1109/TIA.2020.3029125.

[24] Liu B, An M, Wang H, Chen Y, Zhang Z, Xu C, et al. A simple approach to reject DC offset for single-phase synchronous reference frame PLL in grid-tied converters. IEEE Access 2020;8:112297–308. https://doi.org/10.1109/ACCESS.2020.3003009.

[25] Ortega A, Milano F. Comparison of Different PLL Implementations for Frequency Estimation and Control In: Proceedings of the 2018 18th International Conference on Harmonics and Quality of Power (ICHQP), Ljubljana, Slovenia, pp. 1–6,2018. DOI: 10.1109/ICHQP.2018.8378935.

[26] Karimi-Ghartemani M. "Iravani, M.R. Robust and Frequency-Adaptive Measurement of Peak Value". IEEE Trans Power Deliv, 19, 481–489,2004. DOI: 10.1109/TPWRD.2004.824764.

[27] Liu C, Jiang J, Jiang J, Zhou Z. Enhanced grid-connected phase-locked loop based on a moving average filter. IEEE Access 2020;8:5308–15. https://doi.org/10.1109/ACCESS.2019.2963362.

[28] Ranjan A, Kewat S, Singh B. DSOGI-PLL with in-loop filter based solar grid interfaced system for alleviating power quality problems. IEEE Trans Ind Appl 2021;57:730–40. https://doi.org/10.1109/TIA.2020.3029125.

[29] Prakash S, Singh JK, Behera RK, Mondal A. A Type-3 Modified SOGI-PLL with grid disturbance rejection capability for single-phase grid-tied converters. IEEE Trans Ind Appl 2021;57(4):4242–52. https://doi.org/10.1109/TIA.2021.3079122.

Dr. Praveen Bansal is currently working as an Assistant Professor in the Department of Electrical Engineering, MITS, Gwalior (M.P.), India. He obtained his Ph.D. in Electrical Engineering department from DTU Delhi and Master's Degree from MANIT, Bhopal. He has authored/co-authored various scientific articles, book chapters and research articles in indexed international journals and reputed conferences. His research interests include power quality, grid connected systems and multilevel inverters.

Dr. Shishir Dixit is an Associate Professor at Madhav Institute of Technology & Science Gwalior. He joined MITS as Lecturer in July 2003. He obtained his Ph.D. in Electrical Engineering Stream from Maulana Azad National Institute of Technology, Bhopal in 2014, Master's Degree (Design and Production of H. E.E.) from MANIT, Bhopal in 2003, and B.E Electrical from GEC, RDVV, Jabalpur in 1995. He has a total of 19 years of teaching experience. He is also a Member of Professional Societies Like a. LM ISTE b. IET Member c. IEEE Senior Member d. IETE Fellow e. IE(I) Fellow.

Dr. Saket Gupta is currently working as an Assistant Professor in the Instrumentation and Control Engineering Department, Bharti Vidyapeeth College of Engineering, New Delhi, India. He obtained his Ph.D. in Electrical Engineering department from D. T.U, Delhi and M. E. degree in Industrial System & Drives from Madhav Institute of Technology and Science Gwalior, India in 2015. His research interests include Nature Inspired algorithm and their applications in complex optimization problem.

Prof. Majed A. Alotaibi (Member, IEEE) received the B.Sc. degree in electrical engineering from King Saud University, Riyadh, Saudi Arabia, in 2010, and the M.A.Sc. and Ph.D. degrees in electrical and computer engineering from the University of Waterloo, Waterloo, ON, Canada, in 2014 and 2018, respectively. He worked as an Electrical Design Engineer with ABB Saudi Arabia. He is currently an Associate Professor with the Department of Electrical Engineering, King Saud University, and the Director of Saudi Electricity Company Chair for Power System Reliability and Security. He is also serving as the Vice Dean for academic affairs at the College of Engineering, King Saud University. His research interests include power system planning, operation, renewable energy modeling, applied optimization, and smart grid. He has served as a Reviewer for the IEEE TRANSACTIONS ON POWER SYSTEMS and the IEEE TRANSACTIONS ON SMART GRIDS

Dr. Hasmat Malik (Fellow, IETE; Senior Member, IEEE USA) received Diploma in electrical engineering from Aryabhatt Govt. Polytechnic Delhi, B.Tech degree in electrical engineering from Guru Gobind Singh Indraprastha University Delhi, M.Tech degree in electrical engineering from the National Institute of Technology (NIT) Hamirpur, Himachal Pradesh, India, and the Ph.D. degree in Electrical Engineering from Indian Institute of Technology (IIT), Delhi. He has served as an Assistant Professor for more than five years at the Netaji Subhas Institute of Technology (NSIT), Dwarka Delhi, India and 3.5 years as a Postdoctoral scholar with the Berkeley Education Alliance for Research in Singapore (A research center of the University of California, Berkeley, USA) and the National University of Singapore (NUS), Singapore. He is currently a Chartered Engineer (CEng) and a Professional Engineer (PEng). He has published widely in international journals and conferences his research findings related to intelligent data analytics, artificial intelligence, and machine learning applications in power system, power apparatus, smart building & automation, smart grid, forecasting, prediction and renewable energy sources. Dr. Hasmat has authored and co-authored more than 100 research papers, nine books and thirteen chapters in 10 other books, published by IEEE, Springer and Elsevier. He has supervised more than 25 PG students. His principal area of research interests is application of artificial intelligence, machine learning and big-data analytics for renewable energy, smart building & automation, condition monitoring and online fault detection & diagnosis (FDD). Dr. Malik is also a Fellow of the Institution of Electronics and Telecommunication Engineering (IETE), a Senior Member of the IEEE USA, and a member of the Institution of Engineering and Technology (IET), UK, a Life Member of the Indian Society for Technical Education (ISTE), the Institution of Engineers (IEI), India, and the Mir Labs Asia. He received the POSOCO Power System Award (PPSA-2017) for his Ph.D. work for research and innovation in the area of power systems. He also received the Best Research Papers Awards from IEEE INDICON-2015, and the Full Registration Fee Award from IEEE SSD-2012, Germany.

ProfessorFausto Pedro García MárquezHonorary Senior Research Fellow at Birmingham UniversityLecturer at the Postgraduate European InstituteSenior Manager in Accenturedistinguishedwith the pricesHe has published more than 242 papers50booksPrincipal Investigator in 4 European Projects, 8 National Projects, and more than 150 projects for Universities, Companies, etc (Accredited as Full Professor from 2013), Spain, , UK, , and he has been (2013-2014). He obtained his European PhD with a maximum distinction. He has been : Nominate Prize (2022), Gran Maestre (2022), Grand Prize (2021), Runner Prize (2020) and Advancement Prize (2018), Runner (2015), Advancement (2013) and Silver (2012) by the International Society of Management Science and Engineering Management (ICMSEM), First International Business Ideas Competition 2017 Award (2017). (152 JCR: 74-Q1; 39-Q2; 30-Q3; 8-Q4), some recognized as: "Applied Energy" (Q1, IF 9.746, as "Best Paper 2020"), "Renewable Energy" (Q1, IF 8.001, as "Best Paper 2014"); "ICMSEM" (as "excellent"), "Int. J. of Automation and Computing" and "IMechE Part F: J. of Rail and Rapid Transit" (most downloaded), etc. He is author and editor of more than (Elsevier, Springer, Pearson, Mc-GrawHill, Intech, IGI, Marcombo, AlfaOmega,…), >100 international chapters, and 6 patents. He is Editor of 5 Int. Journals, Committee Member more than 70 Int. Conferences. He has been . His main interests are: Artificial Intelligence, Maintenance, Management, Renewable Energy, Transport, Advanced Analytics, Data Science.